



# 3D thermal volume mapping to assess the biological and physical characteristics of olive crops using remote sensing and photogrammetric methods

Nicola Genzano<sup>1</sup> · Roberto Colonna<sup>2</sup>

Received: 22 May 2025 / Accepted: 8 September 2025  
© The Author(s) 2025

## Abstract

Drones, as well as ground-based and satellite platforms, offer the possibility to carry sensors able to obtain timely and precise indications about vegetation health conditions. These systems can serve as tools for agricultural monitoring and the management of crops. Nowadays, Unmanned Aerial Vehicles (UAV) systems are equipped with sophisticated sensors, such as those operating in the Thermal InfraRed spectral range, which can provide indications about the water content of vegetation at very-high spatial resolution. This study explores the feasibility of exploiting drone-based thermal imagery and Structure-from-Motion (SfM) photogrammetry to derive 3-D representations in Precision Agriculture. The health condition of olive trees was evaluated using thermal observations collected by a UAV system over an olive orchard located in the Basilicata region (Southern Italy). Following the SfM pipeline, accurate 2-D/3-D thermal photogrammetric products have been created, and analyzed by means of the Normalized Relative Canopy Temperature (NRCT) index. The goal was to explore how 3D thermal volume analysis can enhance the detection and interpretation of early signs of water stress and related plant health descriptors. Although evident symptoms of stress were not yet visible during the survey, our preliminary results highlight the added value of 3D thermal information over traditional 2D approaches, particularly in capturing spatial variability within individual tree canopies. These findings demonstrate the potential of UAV-based 3D thermal analysis as a valuable tool for advanced monitoring in Precision Agriculture and Smart Farming practices.

**Keywords** Agriculture management · NRCT index, photogrammetry · Structure-from-Motion · UAV thermal imagery · 3D models

## Introduction

In recent years, advances in the Remote Sensing (RS) field are providing new opportunities for agricultural monitoring and opening new scenarios for the management of crops in the context of Precision Agriculture (PA) and Smart Farming (SF) (e.g. Liaghat 2010; Inoue 2020; Sishodia et al. 2020). The use of data coming from Unmanned Aerial Vehicles/

Systems (UAVs/UASs, see Granshaw 2018), as well as those collected by satellite observations (e.g. Gabriele et al. 2025), offers the possibility of studying vegetated areas using remotely-sensed images at suitable spatial, spectral and temporal resolution. Observations provided by UAV surveys are well suited for PA applications (Sishodia et al. 2020), because they can collect very-high spatial resolution imagery in radiometric portions of the electromagnetic spectrum suitable to well understand the vegetation health condition (e.g. Yao et al. 2019). Indeed, such systems can be equipped with multispectral and thermal sensors that can be used for assessing the water needs of the crops or early disease detection, for instance. In addition, modern photogrammetric techniques (Luhmann et al. 2020) allow to generate accurate and geometrically precise 3-D models from drone-based images to reconstruct real-world scenarios aimed to optimize agricultural activities (e.g., Jurado et al. 2022).

✉ Nicola Genzano  
nicola.genzano@polimi.it

<sup>1</sup> Department of Architecture, Built Environment and Construction Engineering (ABCE), Politecnico di Milano, via Ponzio 31, Milano 20133, Italy

<sup>2</sup> Department of Engineering, University of Basilicata, via dell'Ateneo Lucano 10, Potenza 85100, Italy

This study focuses on a specific goal: to evaluate the feasibility of applying 3D photogrammetric reconstructions based on UAV thermal imagery for early detection of water stress in olive orchards, even when visual symptoms are not yet apparent. We conducted a field experiment in a hilly olive grove in Basilicata (Southern Italy), where drones equipped with high-resolution thermal cameras captured overlapping images from multiple stations. These were processed with photogrammetric workflows to generate detailed 3D thermal models of tree canopies. These models allowed for in-depth analysis of temperature variations across the tree canopy, and provided a comprehensive view of temperature distribution, highlighting water-stressed areas with greater precision, rather than the traditional 2-D analyses. Our findings demonstrate that 3D models derived from photogrammetric techniques of thermal imagery may significantly improve water stress evaluation, offering a reliable tool for PA that can help farmers to optimize and better address the traditional crop management procedures.

The manuscript is organized as follows. Section 2 provides a brief overview of the discussed research topics, while information about the testing area, the image acquisition and the adopted methodology are reported in Sect. 3. Achieved results are presented in Sect. 4 and discussed in Sect. 5. Finally, the conclusions and future developments are treated in Sect. 6.

## Background

In recent years, the use of data acquired by UAVs has rapidly increased in the different fields, such as agriculture, forestry, archaeology, environmental monitoring, emergency response, and increasingly in climate-change studies such as glacier and permafrost monitoring. Thanks to their versatility and adaptability, UAV technologies support the traditional RS methods based on satellite and manned aircrafts, to acquire accurate information about Earth's surface and objects above it. In addition, since UAVs can mount sophisticated sensors, which are the miniaturization of commercial tools including multispectral, thermal and hyperspectral cameras, microwave sensors, and Light Detection and Ranging Systems (LiDAR), nowadays, UAVs allows also to capture accurately biophysical and geophysical variables (e.g. Cucho-Padin et al. 2020; Dronova et al. 2021; Lin et al. 2021).

Moreover, advances in image processing and methods development specifically for data collected by UAV systems, for instance, Structure-from-Motion (SfM; e.g. Eltner et al. 2016; Jiang et al. 2020) and Multi-View Stereo (MVS; Furukawa et al. 2015), from one side, have made digital photogrammetry more accessible to a wider range of

users, on the other side have allowed generating accurately 2-D/3-D photogrammetric products, such as orthophoto and texturized models, respectively, useful for assessing and monitoring the investigated scene in different fields (Westoby et al. 2012). Furthermore, recent applications in cryospheric environments, including mapping glacier volume and thickness changes with multi-temporal photogrammetry methods (e.g. Genzano et al. 2024; Eskandari et al. 2024) demonstrate their utility in capturing terrain change in response to climate change.

Among the different fields, agriculture is one sector where data collected by UAV systems were extensively tested and use, and greater benefits are expected. Mapping and classification of crops (Jayakumari et al. 2021), vegetation health status monitoring (Bueren et al. 2015), identification of water (Park et al. 2017) and nutrient deficiency (Adams et al. 2000), irrigation scheduling (Gonzalez-Dugo et al. 2013a, b), disease (Calderón et al. 2013; Terentev et al. 2022) and weed (Kazmi 2011) detection, as well as yield predictions (Feng et al. 2020) are some examples of topic where UAV data are exploited.

Most of the UAV applications in the agricultural fields are based on the use of multispectral cameras, which operate in the visible (VIS) and Near-InfraRed (NIR) spectral range. Such sensors providing information about the spectral absorption and reflection of the vegetation, are very helpful to assess some biological and physical characteristics of crops. A wide overview of UAV applications for monitoring natural and agricultural ecosystems can be found in Manfreda et al. (2018) or in Tsouros et al. (2019), where a critical discussion of the capabilities and limitations of UAV technology in comparison, for example, with spaceborne sensors, it is also treated.

Instead, information about the emitted radiation of the vegetation can be obtained using thermal sensors that usually acquire data in the Long Wavelength Infrared (LWIR) spectral range. Although, less used than the multispectral, such sensors have shown a great potential for agricultural applications about crop health, including plant water stress and plant diseases, as well as assessing crop yield estimation and plant phenotyping. A comprehensive review of the use of drone-based thermal imagery for agriculture purposes can be found in Messina and Modica (2020) and in Jurado et al. (2022).

In particular, Maimaitijiang et al. (2020) exploit data collected by multispectral and thermal sensors aboard UAV systems for estimating soybean grain yield within the framework on the framework of multimodal data fusion and deep learning. Gonzalez-Dugo et al. (2013a, b) used data acquired by a thermal camera mounted on a fixed-wing UAV platform for assessing the water status of different fruit tree species, highlighting the capabilities of such technology

to support water management in PA and to define irrigation strategies. Instead, Santesteban et al. (2017) evaluate the seasonal variability of water status within a vineyard, by analysing drone-based images acquired from a thermal camera at different times during the vineyard veraison stage.

Calderon et al. (2013) evaluate the potentials of different indices retrieved from thermal, multi- and hyperspectral imagery to provide indication about diseases in olive trees due to fungus infection. Among the different indices, the study highlighted the good ability of a thermal index, i.e., Crop Water Stress Index (CWSI; Jackson et al. 1981), to detect in the early stages the disease development. The CWSI thermal index has been demonstrated to be a useful indicator to reveal *Xf* infection months before symptoms were visible in different olive trees in Apulia region (Poblete et al. 2020).

Moreover, advantages for the agricultural sector are also expected by applying modern photogrammetric (i.e., SfM/MVS) 3-D reconstruction techniques with UAV thermal imagery, which allows the generation of accurate three-dimensional models of crops able to provide enhanced information about the vegetation health status, for instance. To better exploit data collected with thermal camera mounted on drone systems, some technological issue should be considered, such as the lower resolution in comparison with RGB imagery, and poor contrast between and within TIR imagery (see Alba et al. 2011). Moreover, also the disadvantage of the use of sensors not very sensitive and accurate (uncooled sensors are typically mounted on UAVs) should be considered (Ribeiro-Gomes et al. 2017).

In the past, to obtain acceptable results either from geometric (i.e., camera calibration and image orientation) and radiometric (i.e., TIR images calibration) points-of-view, several procedures and processing schemes have been proposed. For instance, to properly align the UAV thermal imagery, Turner et al. (2014) proposed a standard procedure, where *i*) a preliminary image selection and their conversion from 8-bit to 16-bit have been applied, *ii*) TIR image alignment is based on onboard GNSS (Global Navigation Satellite System) receiver and image time stamp, *iii*) and finally the image co-registration is performed through ground control points (GCPs), Real-Time-Kinematic (RTK) - GNSS, or RGB orthophotos.

Instead, Maes et al. (2017) with the same purpose have introduced and tested three different procedures that consider camera pre-calibration, an air temperature correction, and an improved estimation of initial image position based on the alignment of RGB images. Although the first two proposed procedures showed a limited impact on the alignment of the TIR dataset, the use of image positions of the RGB imagery for initial estimates of thermal image positions greatly improved thermal image alignment, both in

terms of number of oriented images and in quality (Maes et al. 2017). However, due to the complexity of this issue, there is no consensus about the standard procedure to adopt.

Nevertheless, it is quite obvious that a good thermal reconstruction can be achieved by paying attention to: *i*) planning the flight mission to grant suitable overlap within and across strips (see Pepe et al. 2018); *ii*) flight elevation, which should be maintained constant and operated at moderate flight speed (e.g., less than 5 m s<sup>-1</sup>); *iii*) the use of GCPs, which should be clearly visible in TIR images, should have adequate size (e.g., 50 × 50 cm), and should be made with material with low emissivity (e.g., aluminum sheets) when compared to the adjacent vegetation and other bodies (Boesch 2017).

UAV systems capable of capturing thermal and visible imagery simultaneously enable high-quality thermal reconstructions by leveraging the superior resolution of RGB data to inform TIR processing. Recent advances have led to UAVs equipped with dual sensors, RGB (or multispectral) and thermal, collecting synchronized data streams. Although early methods relied on so-called bi-camera setups (e.g., Alba et al. 2011), more recent developments integrate both datasets through a unified bundle block adjustment (BBA). Initially, this involved manual tie-point selection across modalities (Previtali et al. 2013), but automated approaches now use Structure-from-Motion workflows to align and co-register thermal and visible images accurately (e.g., Conte et al., 2018). These techniques yield coherent 2-D and 3-D thermal models with enhanced geometric precision, facilitating precise thermal mapping in complex environments.

Within this context, here we delve into the capabilities and potentiality of UAV thermal imagery for supporting the management of olive orchards through the generation of specialized 3D outputs, establishing the groundwork for thorough analysis, ongoing monitoring, and effective long-term management.

## Materials and methods

### Study site description

The studied area covers an area of about 1.5 ha (NE (north-east) corner: 40°45'10.6"N, 15°56'10.12"E; SW (south-west) corner: 40°45'08.02"N, 15°56'11.14"E) and it is located in the Cancellara municipality (Basilicata region, Southern Italy) at approx. 600 m orthometric height. The investigated area is characterized by a hilly terrain mainly exposed in the North direction and it is devoted to agricultural purposes. Indeed, the agricultural parcels of such areas are cultivated with olive trees, although they are reported as fruit trees and berry plantations (i.e., 222 class)

in the Corine Land Cover (CLC) 2018 classification (EEA 2018), which is an inventory of land cover and land use thematic classes at European level. CLC 2018 is part of a long-standing European project that monitors and classifies land cover and land use across Europe. It is produced as part of the Copernicus Land Monitoring Service (CLMS; <https://land.copernicus.eu/en>). CLC uses a hierarchical classification system to categorize land cover into 44 distinct classes, organized into broader categories such as artificial surfaces (urban areas), agricultural areas, forests and semi-natural areas, wetlands and water bodies.

## Surveys

### Photogrammetric survey: image block acquisition

The survey was conducted on 6th May 2024 from 13:00 to 14:30 local time. Weather conditions at the time of the survey were stable (air temperature around 21 °C and relative humidity around 40%), as reported by meteorological stations (CFD 2024) located not so far from the investigated area, about 2.8 km towards SW (Cancellara station; 40°43'42"N, 15°55'21"E) and 4.4 km towards NE (Oppido Lucano station; 40°45'50"N, 15°59'8"E). Figure 1 reports a map with the positions of the study area and the

meteorological stations and the plots of the air temperature and the relative humidity measured at the two stations.

A small quadcopter DJI MAVIC 3 T UAV (DJI Combo Mavic 3 thermal universal edition; China, Shenzhen) was used for image acquisition over an area of approx. 7 ha, which was larger than the area under investigation. DJI Mavic 3 T was equipped with two cameras, the first, a 1/2" CMOS sensor that allows to capture 12MP RGB photos with an aperture of f/4.4 (zoom camera), and the second, a thermal camera with a resolution of 640 × 512 pixels in the spectral range 8–14 μm, with a precision ± 2 °C. Consequently, visible and thermal imagery was acquired at the same time over the investigated area. Table 1 summarizes the main geometric and radiometric features of sensors aboard of the used UAV system.

Two different flights conducted with the camera in a nadir position were operated. Both followed a precise flight plan (Fig. 2) at a height of 25 m in according with Italian law for the area under investigation. The flight speed was about 4.9 m/s. Each acquisition took about 25 min, and they were performed by ensuring strips with a rate of image overlap of 80% in both longitudinal sidelap directions. In this manner, the crown of trees was captured under different view angles. The UAV flight planning was conducted using the DJI Terra software (version 3.7.3). A total

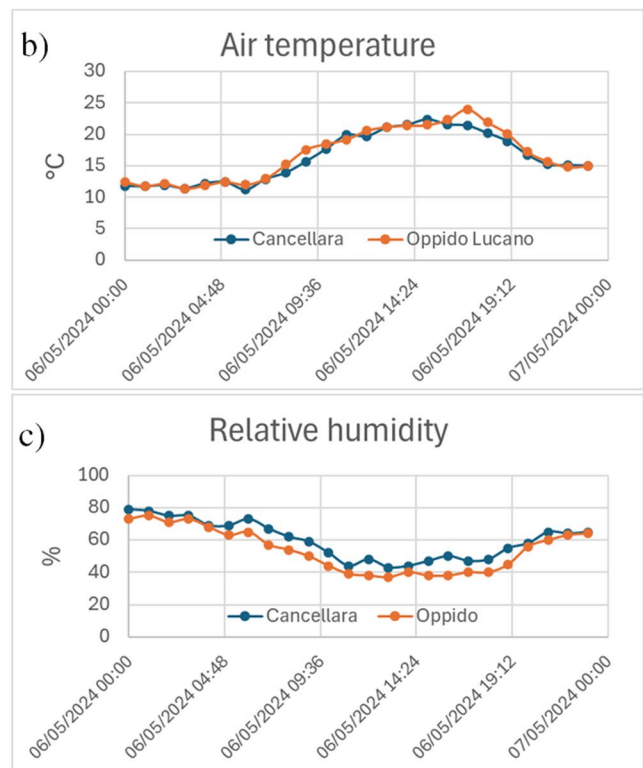
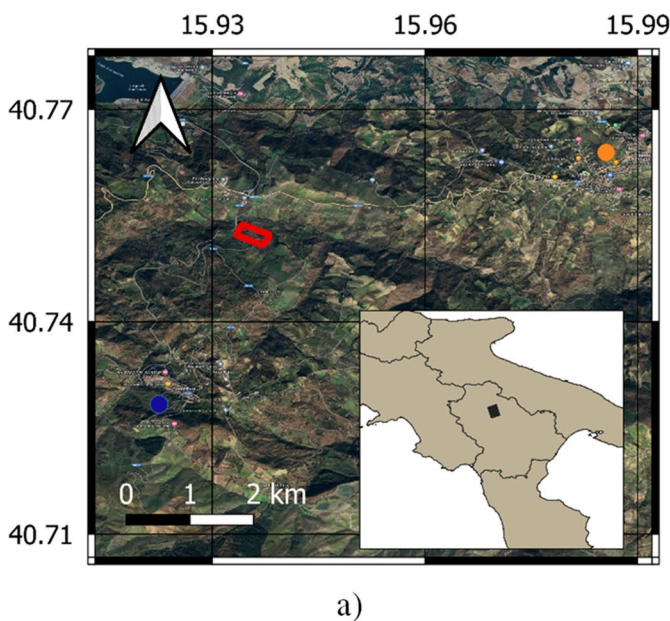


**Fig. 1** On the left side, the localization of the investigated area (**a**). The red rectangle delineates the area acquired by UAV (Unmanned Aerial Vehicles) surveys. Blue and orange points identify the position of two

meteorological stations. On the right side, the plots of air temperature (**b**) and relative humidity (**c**) measured during the whole day (i.e. May 6, 2024) of the UAV survey

**Table 1** Geometric and radiometric features of the visible and thermal cameras mounted on DJI MAVIC 3T UAV

		Visible		Thermal
		Wide camera	Tele camera	
Sensor	Type	CMOS		Uncooled Vox Microbolometer
	Dimension	1/2"		
Lens	FOV	84°	15°	61°
	Equivalent focal length	24 mm	162 mm	40 mm
	Aperture	f/2.8	f/4.4	f/1.0
	Focus	1 m to ∞	3 m to ∞	5 m to ∞
ISO	Min-Max	100 – 25,600		
Resolution (max)		8,000×6,000	4,000×3,000	640×512
Sensitivity				≤50 mk at F1.1
Accuracy				±2°C
Spectral range				8 – 14µm
Measurement range				-20° – 150°C (High Gain)0° – 500°C (Low Gain)



**Fig. 2** The two flight plans considered during the acquisition of visible and thermal images. Cyan rectangles indicate the areas acquired by the UAV surveys and the green lines represent UAV flight paths

of 7,894 images were acquired over the investigated area: 3,947 of them as thermograms in R-JPEG format and the remaining 3,947 as RGB images.

To improve the positioning and accuracy of the outputs, sixteen homemade targets easily recognizable on both RGB and thermal imagery were used. Black and white targets (prepared on polypropylene panels) of 50 × 50 cm size were uniformly distributed in the area to be used as ground control points (GCP) and measured before the flight by means of mobile mapping system (MMS) in a local system.

To make targets more visible also in thermal images, the two white quadrants of the panels were covered with

aluminium sheets of 25 × 25 cm dimension. Since, the aluminium sheets have a lower emissivity, respect to the adjacent objects (e.g., vegetation or soil), the white part of the panel should be easy detectable also the thermal images (they appear as a cold object). Should be noted that, the black and white parts of the target also should represent the thermal extremes of the image at hand. Looking at Fig. 3, where it is shown as appear a target in a thermal image, it is possible note that the maximum (minimum) temperature of the image is located on the white (black) part of the target.

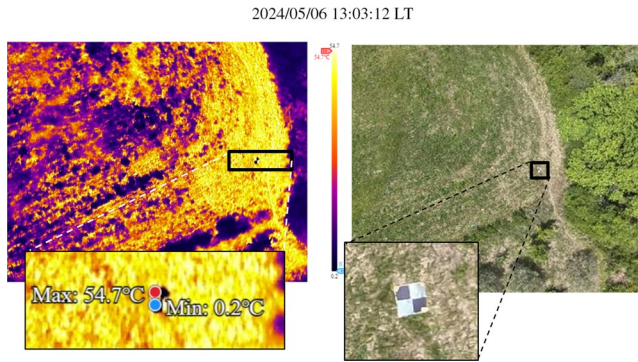


**Fig. 3** Example as the homemade target used as ground control points (GCP) in a thermal (left side) and RGB (right side) images, respectively

### MMS survey

Each GCP was also captured and measured with MMS the ZEB Horizon (GeoSLAM™; <https://geoslam.com/technology/>) to get a first continuous point cloud 3D scenery of the landscape (Fig. 4), and to ensure a more stable connection among the different tests planned for the next months and surveys. A review about this surveying technology can be found in Zhang et al. (2024).

The utilization of an MMS, which has a positional accuracy of  $\pm 1$  to  $\pm 5$  cm, proved indispensable for efficiently acquiring detailed and precisely geo-referenced data from agricultural fields. By significantly reducing manual workload, this technology enhanced overall survey efficiency. It enabled the collection of multidimensional information, including topographic data, high-resolution imagery, and LIDAR data, thereby facilitating comprehensive mapping of both terrain and crop surfaces. The MMS-generated point cloud captures a dense 3D discrete volume of tree crowns, offering fine structural insights beyond what UAV photogrammetry alone can provide. The integration of MMS with UAV data allowed for a more complete and detailed coverage of the area of interest, overcoming spatial and temporal limitations of individual UAV flights. This rich dataset provided a clear depiction of the field's irregular topography and enabled precise identification of critical factors such as elevation variations and crop distribution. By performing UAV-RTK surveys, centimeter-level real-time georeferencing can be achieved, reducing at the same time, the dependency on manually placed ground control points. Moreover, merging the detailed MMS point cloud with the broader UAV photogrammetric cloud can fill canopy occlusions and improve geometric completeness. Together, RTK-UAV surveys and a robust MMS-UAV point cloud fusion will significantly elevate spatial accuracy, model completeness, and effectiveness for agricultural monitoring and canopy structure analysis.

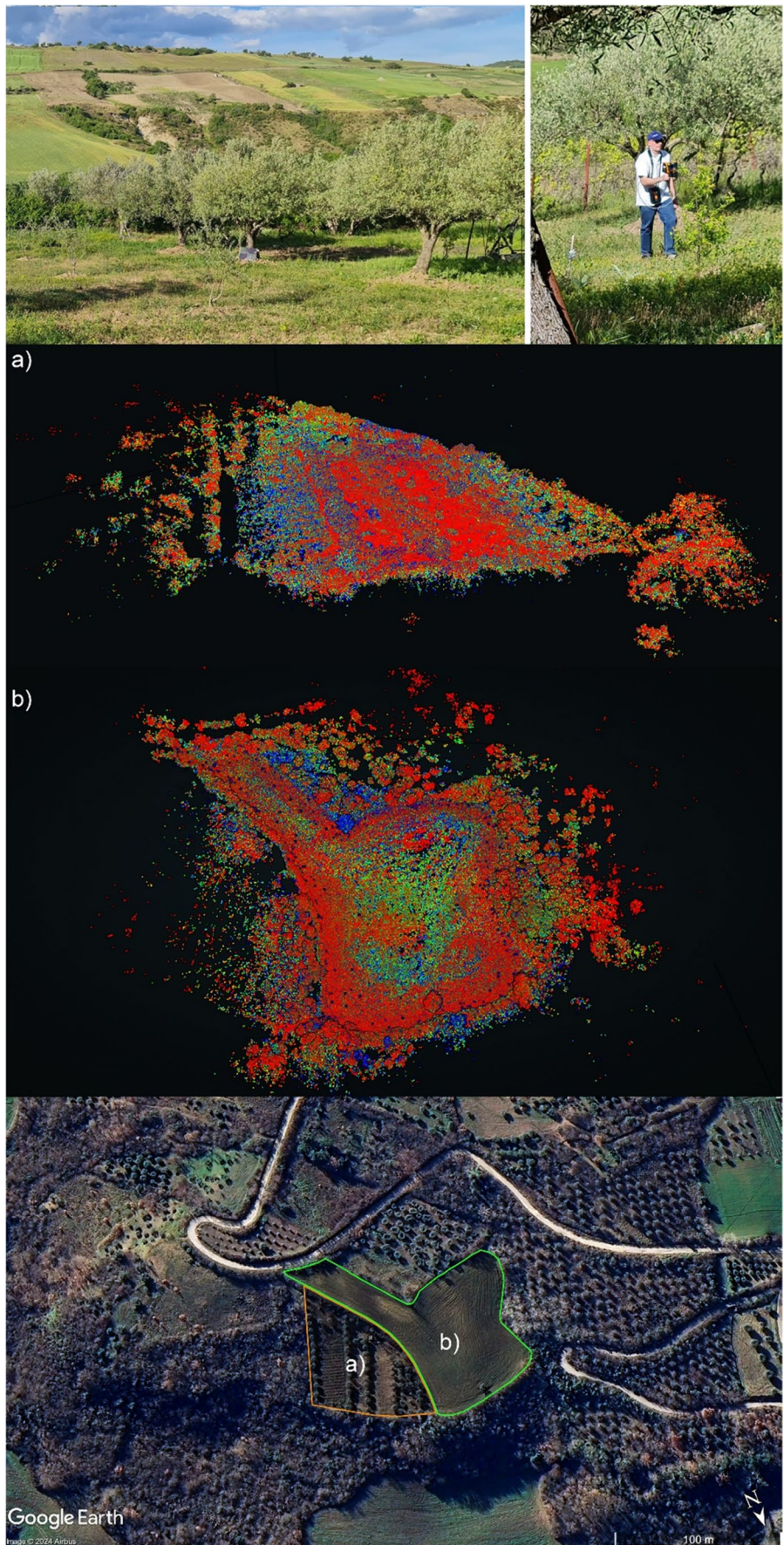
### Image processing

Agisoft Metashape© (version 2.1.0; Agisoft LLC, St. Petersburg, Russia) was used for the photogrammetry processing of both RGB and thermal imagery. Although about 4,000 images have been collected with a high rate of overlap (i.e., 80%), to avoid redundancy of information that can create noise, and consequently complicate the processing, a selection of the images was carried out. Such a strategy also minimized the processing time of the photogramms to be oriented by Structure-from-Motion (SfM) technique (Eltner et al. 2016; Jiang et al. 2020), guaranteeing a good reconstruction of the olive trees present in the investigation area. Two datasets of 434 images each are assembled, the first consisting of RGB photos with a dimension of  $4,000 \times 3,000$  pixels and the second of thermal images with a resolution of  $640 \times 512$  pixels.

Since the DJI MAVIC 3 T UAV system can acquire thermal and visible images simultaneously, it is possible to handle the RGB and TIR imagery at the same time. In this way, by exploiting the information of the RGB images, which have better spatial resolution rather than TIR images, it is expected to have a better reconstruction of the thermal dataset and to obtain accurate 3D thermal products. With this purpose, both image blocks are processed as a multispectral image dataset as follows:

- before performing the image orientation procedure, the thermal images were pre-processed. Since, DJI Mavic 3 T allows the acquisition of radiometric thermal images, which are stored in R-JPEG format, a conversion from Digital Number (DN) to surface temperature in Celsius degree ( $^{\circ}\text{C}$ ) was carried out. The DJI IMAGE PROCESSOR 1.3 (Miro Rava program, [www.miro-rava.com](http://www.miro-rava.com)) was used for processing the thermal data by considering the object emissivity, atmospheric conditions and distance between the sensor and the target object and in according to those settled during the flight planning phase (e.g. emissivity  $\varepsilon=0.95$ ). A comprehensive discussion on the theoretical aspects at the basis of DN to surface temperature conversion procedure adopted in our study can be found in the work of Usamentiaga et al. (2014);
- images were aligned by means of bundle block adjustment (BBA), where the key points were identified and matched to each other on the images at hand, resulting in a set of tie points visible on multiple images. Moreover, for each image exterior orientation parameters were estimated, together with the camera inner orientation and additional calibration parameters (see Luhmann et al. 2020). Exploiting the GCP coordinates coming from the MMS GEOSLAM LiDAR campaign, targets were positioned on the images at hand to optimize and to georeferenced the project in a local reference system as a first step, and then

**Fig. 4** LiDAR data obtained through a mobile mapping system (ZEB Horizon): (a) olive orchard, (b) wheat field. ZEB point clouds are coloured from blue to red in accord to their intensity. LiDAR scans proved useful for georeferencing and completing the aerial photogrammetric data of the surveyed area. Credits for the background image at the bottom go to Google Earth®



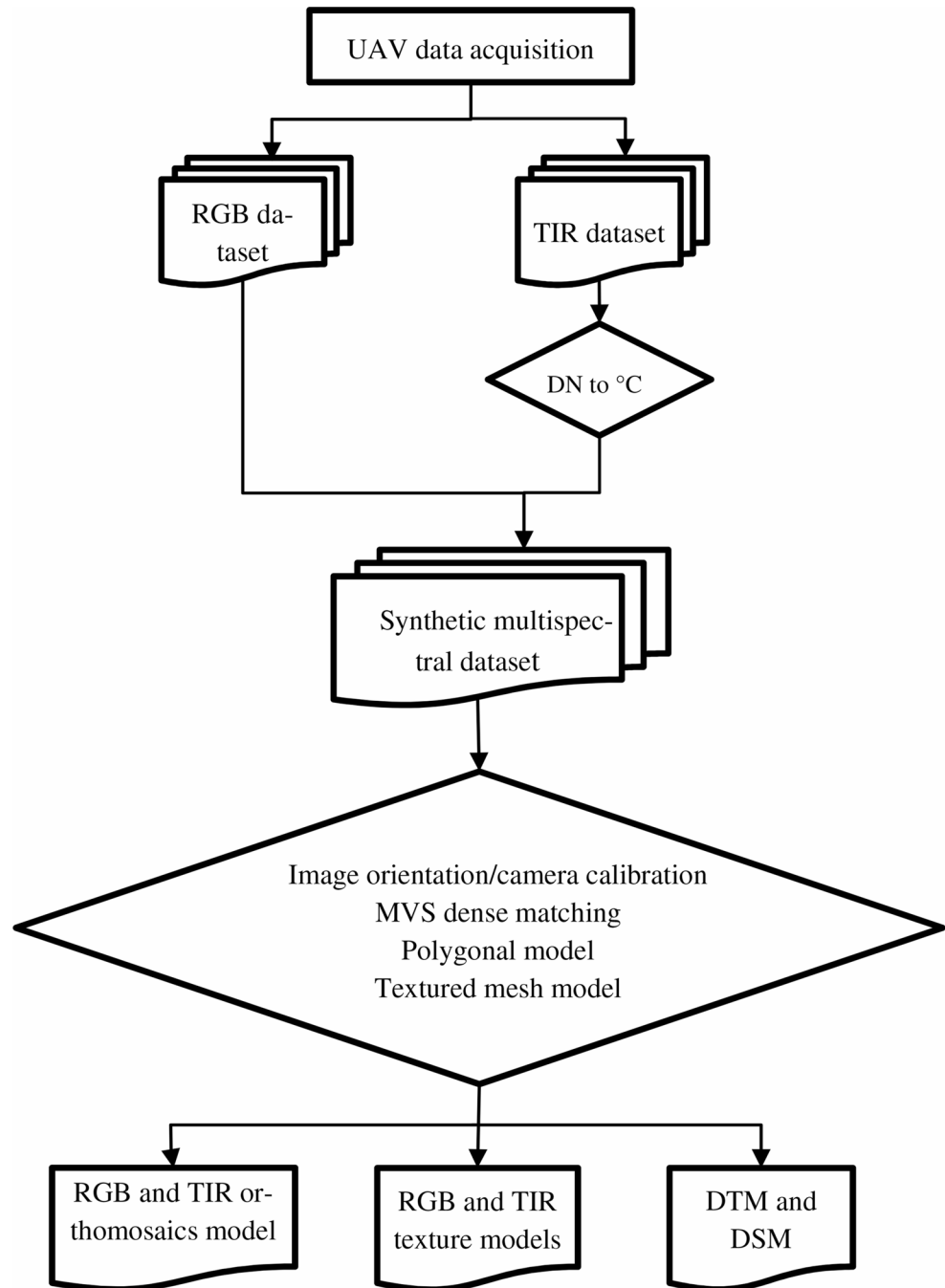
in a geographical reference system exploiting information coming from available and free-accessible aerial ortho-photo (e.g. <https://rsdi.regione.basilicata.it/viewGis/?project=C5E7A17D-92E8-4DAB-FF83-D79F568CFE6F>);

- based on the parameters estimated during the BBA, a dense point cloud was generated through Multi View Stereo (MVS) matching. Inconsistent points were manually deleted after point cloud generation, and eventually, then a polygonal model (3-D mesh) was generated from

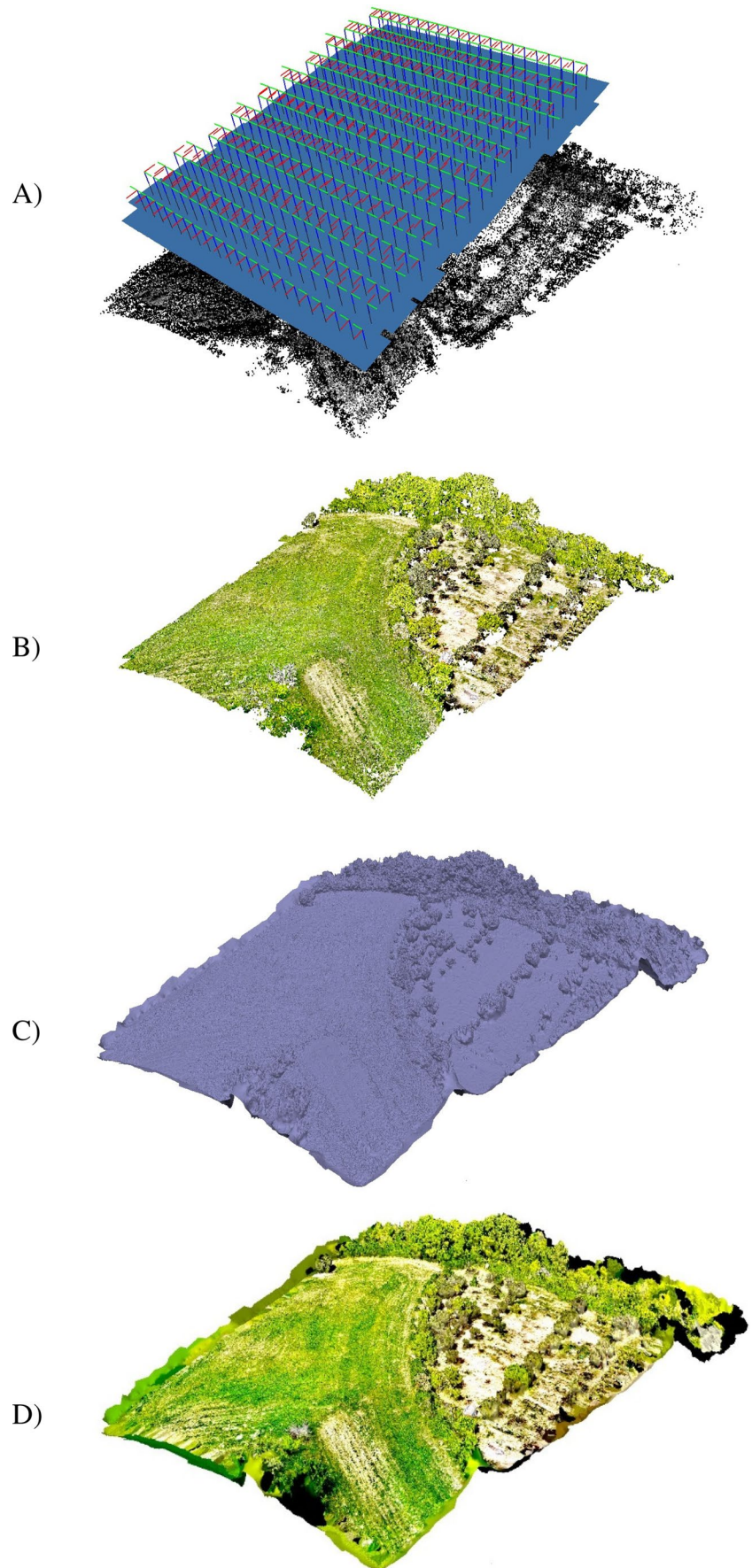
point clouds. By this way, bi-dimensional (e.g., ortho-mosaic) and tri-dimension (e.g., digital surface model, high-resolution photorealistic digital representations) products of the test site were obtained.

Figure 5 reports the schematic workflow of the UAV image processing. Instead, Fig. 6 shows the intermediate and final outputs of the UAV-photogrammetry process and Table 2 reports a summary of these outputs.

**Fig. 5** Flowchart representing the complete UAV photogrammetry workflow



**Fig. 6** Intermediate and final outputs of the UAV-photogrammetry process (from top to bottom): sparse point cloud made up of tie points generated after image orientation and camera poses (A), dense cloud (B), mesh (C), and textured model (D)



**Table 2** Summary of the intermediate and final outputs of the UAV-photogrammetry outputs

Aligned synthetic multispectral images (RGB+TIR)	434
Tie points	460,842 (350,512 on RGB images, 109,773 on TIR images and 557 on both datasets)
Dense point clouds	40,544,813
3D mesh faces	13,611,924

## Thermograms post-processing procedures

In pursuit of a detailed understanding of the spatial dynamics of agricultural fields and fruit trees studied thorough analysis of the generated thermal products was paramount. UAV thermal sensors, like their ground-based and satellite counterparts, emerged as pivotal tools offering crucial insights into crop health. These sensors provide comprehensive data, encompassing assessments of vegetation water stress, detection of plant diseases, and even estimations of crop yields.

The utility of UAV thermal sensors lies in their ability to capture high-resolution thermal imagery from vantage points that ground-based methods cannot easily access. This aerial perspective allows for detailed mapping of temperature differentials across fields and orchards, revealing possible early signals of vegetation stress and disease that may not be perceptible at ground level. By overlaying these thermal images with geospatial data, researchers and farmers can pinpoint specific areas of concern and tailor management strategies accordingly. This comprehensive understanding allows for the development of robust models and indices that predict crop responses to varying environmental conditions with greater accuracy.

In the past years, several methodologies and indices were proposed for understanding the thermal behaviour of vegetation using thermal images. Most of them take into account not only the plant temperature but also meteorological conditions (e.g., air temperature, atmospheric humidity). One of the temperature-based indices extensively used for crop monitoring is the Crop Water Stress Index (CWSI) proposed by Idso et al. (1981) and Jackson et al. (1981). It should be noted that CWSI index is derived from infrared thermometers and in the original formula proposed by Jackson et al. (1981) the differences between leaf and air temperatures were considered. In our study, we have no information about the air temperature of the test site, but we only know the air temperature measured in meteorological stations not so far from the investigated area, therefore we chose to use the Normalized Relative Canopy Temperature (NRCT) index (Elsayed et al. 2015, 2017). Should be noted

that the thermal images were captured in a short period, and analysing a single daily thermogram, to avoid errors due to a wrong estimation of air temperatures, we prefer to use an index that works only on information inferable on the image at hand. The NRCT was calculated based on the following equation:

$$NRCT = \frac{T_{leaf} - T_{min}}{T_{max} - T_{min}}$$

where  $T_{leaf}$  is leaf surface temperature,  $T_{min}$  and  $T_{max}$  are the lowest and highest temperature of the investigated tree, respectively. The NRCT index can assume values that range between 0 and 1 and can be assumed as directly proportional to the water stress level of the analysed plant.

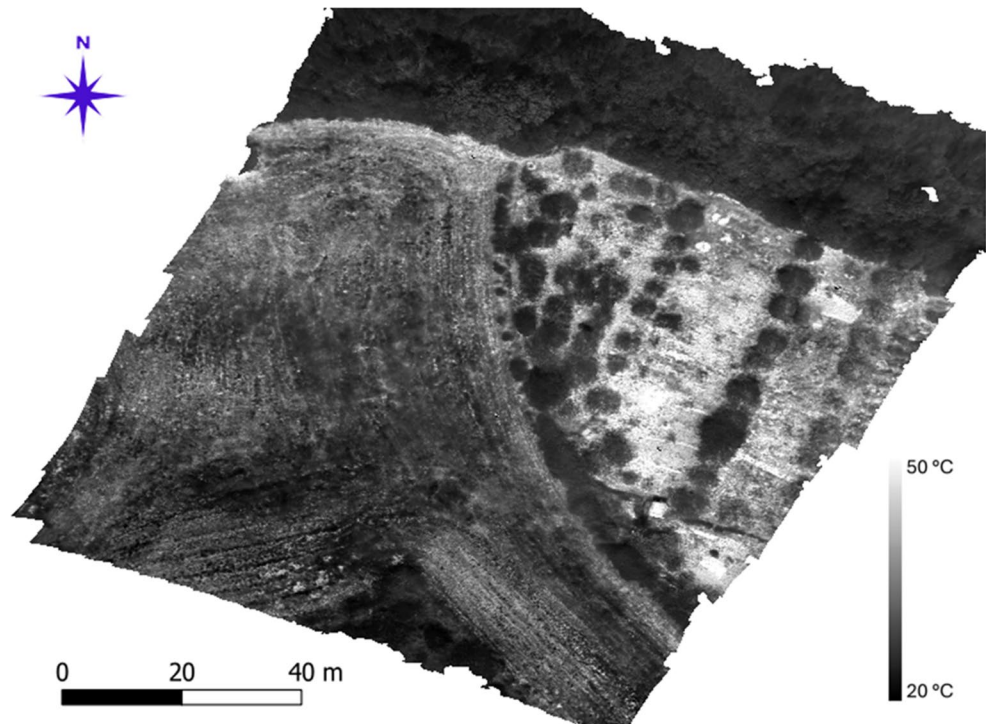
Taking in mind the CWSI index, it should be noted that  $T_{min}$  matches to  $T_{wet}$ , i.e., the wet leaf temperature, which corresponds to a leaf with stomata fully open. Instead,  $T_{max}$  matches to  $T_{dry}$ , i.e., the dry-leaf temperature, which is the temperature of a non-transpiring leaf (the stomata are closed). If not properly estimated, the values of  $T_{min}$  and  $T_{max}$  can lead to a wrong estimation of the NRCT index. As shown in Messina and Modica (2020) therein, different methods were proposed to estimate the temperature where the plant transpires (lower limit) and not transpire (upper limit). Moreover, when implementing the NRCT on thermal imagery (e.g., from satellite or drone), the problem of the ‘mixed-pixel value’ should be considered. Here, to avoid the plant temperature being erroneously compared with the soil temperature, we exploit photogrammetric 3-D models for separating the soil pixels from plant pixels.

## Results

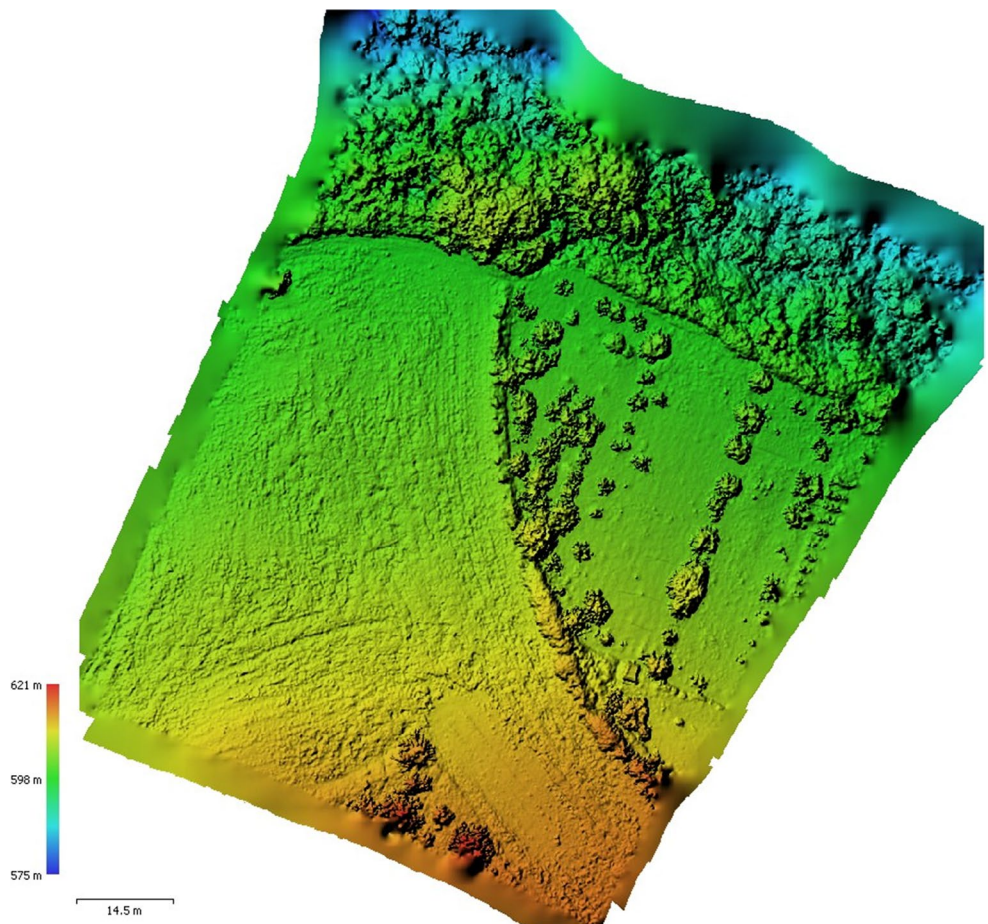
Drone-based high-resolution RGB imagery was mainly used to obtain indications about the canopy structure, whereas thermal imagery was used to obtain indications about the vegetation health status. To this aim, we generate different kinds of products, like:

- high-resolution thermal orthoimages (Fig. 7), it provides an aerial perspective on temperature variations across agricultural landscapes, opportunely treated it can highlight thermal anomalies indicative of plant stress, disease presence, and overall crop vigour;
- Digital Surface Model (DSM; Fig. 8), it provides information about the variation of altitude of the landscape and objects above it. Here, we use this kind of product to retrieve information about the crown of olive trees;
- three-dimensional thermographic output such as a thermic texturized polygonal model (Fig. 9). It reconstructs

**Fig. 7** Thermal orthomosaic of the investigated area



**Fig. 8** Digital Surface Model of the investigated area



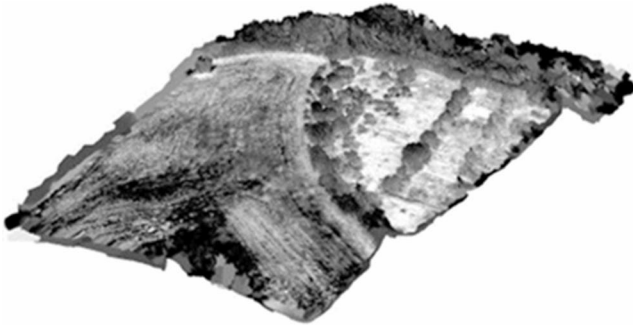
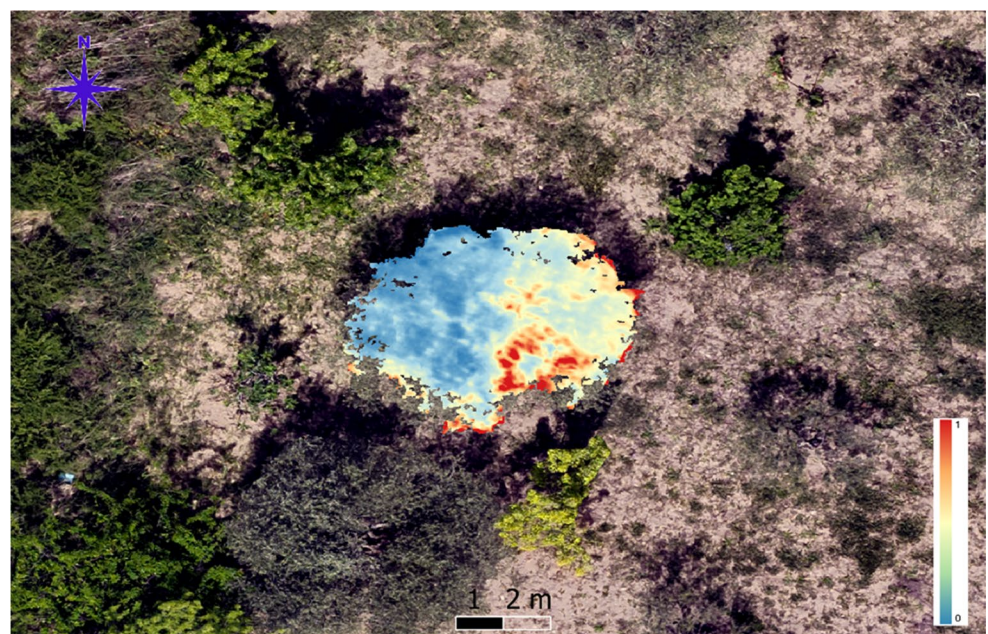


**Fig. 9** Thermal textured 3D model of the investigated area

the agricultural test site in three dimensions, and incorporating thermal textures can facilitate the evaluation of the thermal status of the analysed crops, if properly managed.

On this basis, olive trees present in the study area were analysed by implementing NRCT index on the thermographic product, even if at the time of the survey olive trees did not show evidence of stress clearly visible. The geometric information of vegetation was obtained from the generated DSM. This delineation should ensure to exclude background pixels from the estimation of the minimal and maximum temperature of the olive plant at hand. Then, from the orthomosaic TIR-based have been extracted information about the temperature of the olive trees and the NRCT index was computed per each plant. In Fig. 10 as an example is reported, showing a close view of a NRCT map of an olive tree. Here, it is possible to note that the majority part of the canopy has low values of the NRCT index which means the plant is transpiring. However, some parts of the canopy

**Fig. 10** Example of a NRCT (Normalized Relative Canopy Temperature) map for an olive tree. Blue and cyan colours represent the parts of the canopy in no water stress condition, instead orange and red colours depict those parts of the olive plant in apparently water stress condition



show medium-high values of the NRCT index (orange and red pixels), which could suggest initial signs of vegetative stress. It should be noted that these pixels are located prevalently in the external part of the crown of the tree. This circumstance suggests that the effect of background soil is not completely removed by using only the 2-D product to discern the canopy structure from the soil. For such reason, the added value of 3-D products has been exploited, either for analysis and interpretation purposes, to better delineate the crown of the tree.

Following the same steps of the 2D analysis, olive trees have been also analysed by means of 3-D photogrammetric products. From the generated dense-cloud product, the 3-D point clouds classified as vegetation, which represent the canopy structure, were extracted. Then, the TIR textured polygonal model was used to obtain information about the temperature of the olives canopy, and finally, the NRCT index was computed. Figure 11 reports an example of NRCT index three-dimensional reconstruction.

Looking at Fig. 11, where the olive tree shown in Fig. 10 was considered, it is possible to note that the 2D and 3D representations of the NRCT index of the same plant are in good agreement. This means that any possible artifacts were not generated during the computation of the NRCT index in the 3-D domain. As for the 2-D analysis, also the 3-D analysis does not highlight signs of water stress for such a plant.

The 3-D product helps to better evaluate the performed analysis. Indeed, those parts of the canopy identified in the 2-D analysis possibly in a water stress (i.e., orange and red pixels in Fig. 11), in the 3-D domain seem related to the 'mixed-pixel value' issues, because their position is located

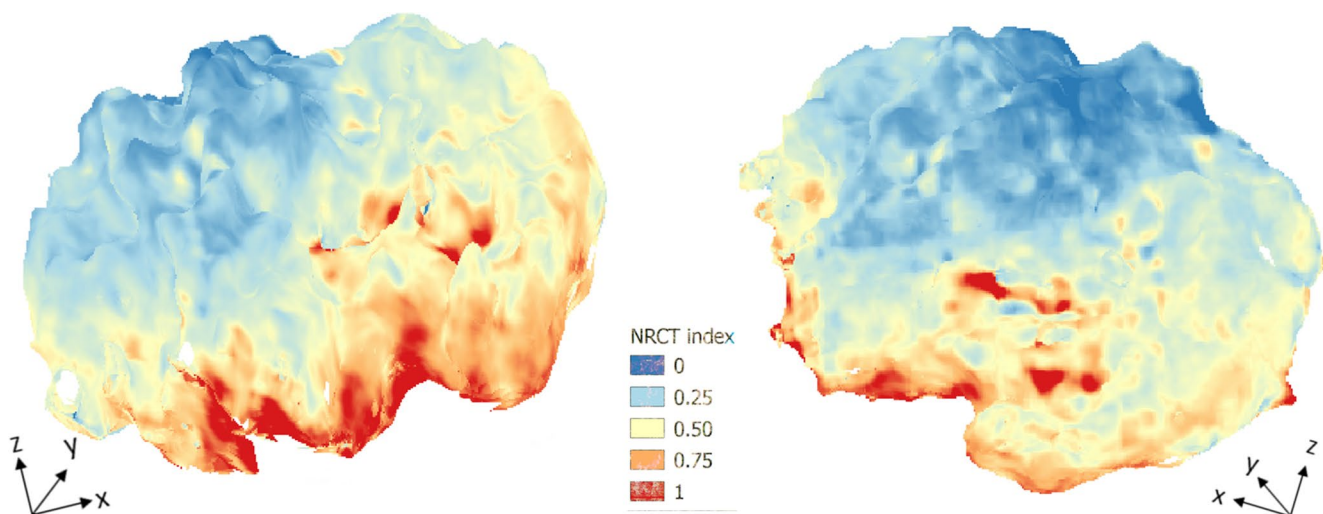


**Fig. 11** Three-dimensional view of the crown of the olive tree shown in Fig. 10 depicted in accordance with the NRCT index

on the side part of the plant rather than on the top of the canopy, where the contribution of the soil temperature could be prevalent in comparison with those of the vegetation.

A similar approach was also performed on the other olive plants present in the study area. Some initial considerations can be drawn based on the achieved results. First, this analysis does not highlight obviously signs of water stress or signs of diseases on the analysed olive trees. However, further analyses, in particular in the temporal domain, needed to better understand the health status of such plants during the different growth stages. Instead, from the methodological point-of-view based on a visual inspection of thermal products the added value of a three-dimensional analysis in comparison with 2D is confirmed. Indeed, when properly treated the 3-D products (e.g., the texturized thermal model) can be processed without the generation of artifacts, providing a more comprehensive vision of the vegetative status of the crop in the interpretation phase.

## Discussion

In the perspective of sustainability in agriculture, both environmental and economic, rural areas, and particularly those devoted to agricultural purposes, need to be continuously assessed and monitored, not only to overcome some global challenges such as climatic changes, land degradation and the food security for instance, but also to help the farmers into the crops management. In this context, remote sensing technologies (aerial or satellite) represent a valid tool able to monitor at different spatial and temporal resolutions those regions devoted to agricultural purposes, providing useful information about yield production, crop diseases, weed detection and so on.

In this paper, we focus attention on the use of drone systems that for their own features (e.g. flexibility, versatility, adaptability) lend themselves well to investigating small areas, such as the agricultural fields, at very high spatial resolution. Nowadays, since such kinds of systems are equipped with sensors, which are the miniaturization of more sophisticated multi-, hyper-spectral and thermal sensors, can provide unique, timely and efficient information on the vegetated areas. In particular, we have evaluated the use of the UAV thermal imagery for assessing the health condition of olive trees and we have exploited the advantage of the photogrammetric methods to better analyse and understand in the tri-dimensional domain the vegetative status of considered crop.

Although UAV thermal images, when compared with UAV multispectral images, can apparently show some drawbacks (e.g. Lopez et al. 2021), mainly related to technological issues, such as the low resolution and the poor contrast. In addition TIR data can be affected by environmental factors, e.g. humidity in the atmosphere, that lead to time expensive data processing procedures and/or to the necessity to perform specific field measurements (e.g. use of hand thermo-camera). Our preliminary test carried out by using a UAV thermic survey confirms the great potentiality of such technology to assess the vegetation health status and to furnish useful indication for the crops management.

Of course, and in particular, in the perspective of a multi-temporal analysis based on UAV thermal images, the above-mentioned limitation due to environmental factors should be better addressed and attenuated. For instance, when working with thermal images acquired in different periods of the year and/or in different hours of the day, it is preferable to use TIR images accurately calibrated, as shown in Lamberini et al. (2022), where possible sources of noise (e.g. the

temperature and humidity of the air, the background soil temperature) are considered and consequently reduced. On the contrary, when images were collected in a short period, as in this study, and in order to obtain preliminary and fast indications about the vegetation health status, which can reveal early signs of diseases, our finding shows that thermal images, at least in the first analysis, can be analysed by adopting methods and indices that work in the spatial domain, such the NRCT index.

From the geometrical point of view, since such analysis is a preliminary test where we try to assess different aspects to exploit in future monitoring campaigns, handling RGB and thermal imagery as a synthetic multispectral dataset, rather than processing the two datasets separately as in most frequent adopted workflows (e.g. Webster et al. 2018), proved itself to be a convenient solution, which allowed us to generate an accurate thermographic 3D model. However, in the perspective of a monitoring campaign, the use of the DJI RTK (Real-Time Kinematics) module should increase the geometrical accuracy of 3D models and facilitate their integration with data coming from other sources (e.g. satellite data) in a common UTM reference system.

Moreover, the achieved results confirm the potential advantages of the usage of the three-dimensional photogrammetric products to better understand the health condition of the olive trees considering the volume consistencies not just the two-dimensional preferential top view. In this context, the possibility of acquiring at the same time panchromatic RGB and TIR images has demonstrated a great advantage for the reconstruction of the canopy structure. By using dense cloud points obtained by RGB-TIR image processing as an input for the extraction of the vegetation temperature from thermographic products, we were able to investigate only the canopy temperature, estimating at best the temperatures where the plant both transpires (lower limit) and not transpires (upper limit). Consequently, the NRCT index has been correctly computed in the tri-dimensional domain without the generation of artifacts. The 3D reconstruction allows us to better understand and accurately evaluate the indications furnished using 2D products. For instance, during the generation of bi-dimensional products, such as orthomosaics, it is possible that mixed pixels, i.e. vegetation and soil, usually located in the external portions of the canopy structure, can generate small portions apparently in water stress conditions. Therefore, having an accurate 3D vision of the crown of the tree can facilitate the evaluation of these kind of situations.

Achieved results encourage us to exploit the advantages of tri-dimensional reconstructions based on photogrammetric methods and techniques applied to data collected by UAV sensors operating in those portions of the electromagnetic spectrum suitable to study the vegetation, such as Near

InfraRed (NIR) and Short-Wave InfraRed (SWIR). Finally, benefits are expected by the integration of observations coming from thermal, multi- and hyper-spectral cameras, as well as monitoring of the vegetation during different phenological phases, providing a more comprehensive view of agricultural fields for better management and adopting sustainable agricultural practices.

## Conclusions

This paper discussed the benefits furnished by drone-based 3D products for supporting agricultural management practices, with a particular focus on the water stress condition of olive trees. We have performed a field experiment in olive groves located in a hilly region of the Basilicata (Southern Italy), which involved UAV equipped with high-resolution thermal and RGB cameras. We have provided a complete description of the adopted approach/procedures from the image acquisition planning to data processing, as well as a critical interpretation/discussion of the achieved results.

In this study, to obtain a good reconstruction of thermal imagery, RGB and thermal datasets were processed simultaneously as a synthetic multispectral dataset. Indeed, thanks to the adopted processing strategy has been possible to reconstruct in a better manner the thermal canopy structure of olive trees in the three dimensions. As a consequence, it has been possible to estimate at best the temperatures where the plants transpire and not transpire, and evaluate better the water condition of the investigated plants.

Although this test represents a preliminary step toward the establishment of a monitoring system based on both ground- and aerial- (e.g. UAV and satellite) sensors, and aimed to assess the health condition of crops, such as the olive orchards, the achieved results confirm the added-value of a 3D approach to better evaluate the indications coming from an UAV thermal survey. On the other hand, looking toward a crop monitor campaign to be carried out during the different growth stages, occur to define a better strategy for correcting the thermal images for the effects of the environmental factors and the emissivity of the different objects present at the ground surfaces, as well as the adoption of an automatic method for separating individual plants.

By incorporating the DJI RTK module during UAV image acquisition, centimeter-level real-time georeferencing will be achieved, dramatically reducing also reliance on manually placed ground control points and enabling seamless temporal integration between UAV 3D products and other ground- and satellite-based datasets within a common UTM coordinate system. Additionally, it will allow a merge between the high-density MMS point cloud and the broader UAV photogrammetric cloud, filling

canopy occlusions and enhancing geometric completeness, resulting in richer and more structurally coherent 3D models. Together, deploying RTK-enabled UAV surveys and executing robust MMS–UAV point-cloud fusion will significantly enhance spatial accuracy, model completeness, and overall effectiveness in agricultural monitoring and canopy structure analysis.

Our findings have demonstrated that the use of 3D thermal images offers a reliable tool for adopting PA practices, which can help farmers optimize and better schedule the traditional crop management procedures, as well as can contribute to overcome some global challenges, e.g. land degradation and the food security, and reach a more sustainability in agriculture field.

**Acknowledgments** The authors would like to thank the prof. Raffella Brumana of Politecnico di Milano and prof. Valerio Tramutoli of University of Basilicata for providing instrumentations necessary for the field survey. Authors would like to thank prof. Marco Scaioni for the useful suggestion provided about the UAV-data processing.

**Author contributions** All authors conceived and defined the research. N.G. defined the methodology, conducted analyses and wrote the original draft. R.C. and N.G. collected the data. All authors reviewed the manuscript.

**Funding** Open access funding provided by Politecnico di Milano within the CRUI-CARE Agreement. The authors declare that no funds were received to conduct this research study.

**Data availability** The data that support the findings of this study are available from the corresponding author, upon reasonable request.

## Declarations

**Competing interests** The authors declare no competing interests.

**Open Access** This article is licensed under a Creative Commons Attribution 4.0 International License, which permits use, sharing, adaptation, distribution and reproduction in any medium or format, as long as you give appropriate credit to the original author(s) and the source, provide a link to the Creative Commons licence, and indicate if changes were made. The images or other third party material in this article are included in the article's Creative Commons licence, unless indicated otherwise in a credit line to the material. If material is not included in the article's Creative Commons licence and your intended use is not permitted by statutory regulation or exceeds the permitted use, you will need to obtain permission directly from the copyright holder. To view a copy of this licence, visit <http://creativecommons.org/licenses/by/4.0/>.

## References

Adams ML, Norvell WA, Philpot WD, Peverly JH (2000) Toward the discrimination of manganese, zinc, copper, and iron deficiency in Bragg soybean using spectral detection methods. *Agron J* 92(2):268–274

- Alba MI, Barazzetti L, Scaioni M, Rosina E, Previtali M (2011) Mapping infrared data on terrestrial laser scanning 3D models of buildings. *Remote Sens* 3(9):1847–1870
- Boesch R (2017) Thermal remote sensing with UAV-based workflows. *Int Arch Photogramm Remote Sens Spat Inf Sci* 42:41–46
- Bueren S, Burkart A, Hueni A, Rascher U, Tuohy M, Yule I (2015) Deploying four optical UAV-based sensors over grassland: challenges and limitations. *Biogeosciences* 2:163–175
- Calderón R, Navas-Cortés J, Lucena C, Zarco-Tejada P (2013) High-resolution airborne hyperspectral and thermal imagery for early detection of verticillium wilt of Olive using fluorescence, temperature and narrow-band spectral indices. *Remote Sens Environ* 139:231–245
- Centro Funzionale Decentrato (CFD) Protezione Civile Regione Basilicata. Available online: <https://centrofunzionale.regione.basilicata.it/it/> (accessed on 24.07.2024)
- Conte P, Girelli VA, Mandanici E (2018) Structure from motion for aerial thermal imagery at city scale: pre-processing, camera calibration, accuracy assessment. *ISPRS J Photogramm Remote Sens* 146:320–333
- Cucho-Padín G, Loayza H, Palacios S, Balcazar M, Carbajal M, Quiroz R (2020) Development of low-cost remote sensing tools and methods for supporting smallholder agriculture. *Appl Geomat* 12:247–263
- Dronova I, Kislik C, Dinh Z, Kelly M (2021) A review of unoccupied aerial vehicle use in wetland applications: emerging opportunities in approach, technology, and data. *Drones* 5:29
- Elsayed S, Rischbeck P, Schmidhalter U (2015) Comparing the performance of active and passive reflectance sensors to assess the normalized relative canopy temperature and grain yield of drought-stressed barley cultivars. *Field Crops Res* 177:148–160
- Elsayed S, Elhoweity M, Ibrahim HH, Dewir YH, Migdadi HM, Schmidhalter U (2017) Thermal imaging and passive reflectance sensing to estimate the water status and grain yield of wheat under different irrigation regimes. *Agric Water Manage* 189:98–110
- Eltner A, Kaiser A, Castillo C, Rock G, Neugirg F, Abellán A (2016) Image-based surface reconstruction in geomorphometry—merits, limits and developments. *Earth Surf Dyn* 4(2):359–389
- Eskandari R, Genzano N, Fugazza D, Scaioni M (2024) Investigation on Miage/Brenva glaciers in the Alps from 50s to-date based on remote-sensing data. *Int Arch Photogramm Remote Sens Spat Inf Sci* 48(3):147–154. <https://doi.org/10.5194/isprs-archives-XLVIII-3-2024-147-2024>
- European Environment Agency (EEA) Corine Land Cover (CLC) 2018, Version 20b2. Release Date: 21-12-2018. Available online: <https://land.copernicus.eu/pan-european/corine-land-cover/clc2018>
- Feng A, Zhou J, Vories E, Sudduth K, Zhang M (2020) Yield estimation in cotton using UAV-based multi-sensor imagery. *Biosyst Eng* 193:101–114
- Furukawa Y, Hernandez C (2015) Multi-View stereo: A tutorial. *Found Trends<sup>®</sup> Comput Graphics Vis* 9(1–2):1–148
- Gabriele M, Brumana R, Genzano NA (2025) Site-specific survey for EO-based phenological monitoring in regenerative agriculture within LULUCF framework. *European Journal of Remote Sensing* 58(1):2515491 <https://doi.org/10.1080/22797254.2025.2515491>
- Genzano N, Fugazza D, Eskandari R, Scaioni M (2024) Multitemporal structure-from-motion: a flexible tool to cope with aerial blocks in changing mountain environment. *Int Arch Photogramm Remote Sens Spat Inf Sci* 48:99–106. <https://doi.org/10.5194/isprs-archives-XLVIII-2-2024-99-2024>
- Gonzalez-Dugo V, Zarco-Tejada P, Nicolás E, Nortes P, Alarcón J, Intrigliolo D, Fereres E (2013a) Using high resolution UAV thermal imagery to assess the variability in the water status of ve fruit tree species within a commercial orchard. *Precis Agric* 14(6):660–678

- Gonzalez-Dugo V, Zarco-Tejada P, Nicolás E, Nortes PA, Alarcón JJ, Intrigliolo DS, Fereres EJPA (2013b) Using high resolution UAV thermal imagery to assess the variability in the water status of five fruit tree species within a commercial orchard. *Precis Agric* 14:660–678
- Granshaw S (2018) RPV, UAV, UAS, RPAS ... or just drone? *Photogramm Rec* 33(162):160–170
- Idso SB, Jackson RD, Pinter PJ, Reginato RJ, Hatfield JL (1981) Normalizing the stress-degree-day parameter for environmental variability. *Agric Meteorol* 24:45–55
- Inoue Y (2020) Satellite-and drone-based remote sensing of crops and soils for smart farming—a review. *Soil Sci Plant Nutr* 66(6):798–810
- Jackson RD, Idso SB, Reginato RJ, Pinter PJ (1981) Canopy temperature as a crop water stress indicator. *Water Resour Res* 17:1133–1138
- Jayakumari R, Nidamanuri RR, Ramiya AM (2021) Object-level classification of vegetable crops in 3d lidar point cloud using deep learning convolutional neural networks. *Precis Agric* 22:1617–1633
- Jiang S, Jiang C, Jiang W (2020) Efficient structure from motion for large-scale uav images: a review and a comparison of Sfm tools. *ISPRS J Photogramm Remote Sens* 167:230–251
- Jurado JM, López A, Pádua L, Sousa JJ (2022) Remote sensing image fusion on 3D scenarios: a review of applications for agriculture and forestry. *Int J Appl Earth Obs Geoinf* 112:102856
- Kazmi W, Bisgaard M, Garcia-Ruiz FJ, Hansen KD, Cour-Harbo A (2011) la Adaptive surveying and early treatment of crops with a team of autonomous vehicles. In *Proceedings of the 5th European Conference on Mobile Robots ECMR 2011* (pp. 253–258)
- Lambertini A, Mandanici E, Tini MA, Vittuari L (2022) Technical challenges for multi-temporal and multi-sensor image processing surveyed by UAV for mapping and monitoring in precision agriculture. *Remote Sens* 14:4954
- Liaghat SBS (2010) A review: the role of remote sensing in precision agriculture. *Am J Agric Biol Sci* 5(1):50–55
- Lin YC, Liu J, Fei S, Habib A (2021) Leaf-off and leaf-on UAV lidar surveys for single-tree inventory in forest plantations. *Drones* 5(115):23
- Lopez A, Jurado JM, Ogayar CJ, Feito FR (2021) An optimized approach for generating dense thermal point clouds from UAV-imagery. *ISPRS J Photogramm Remote Sens* 182:78–95
- Luhmann T, Robson S, Kyle S, Boehm J (2020) Close-range photogrammetry and 3D imaging. *Walter de Gruyter GmbH & Co KG.*, p 822
- Maes WH, Huete AR, Steppe K (2017) Optimizing the processing of UAV-based thermal imagery. *Remote Sens* 9:476
- Maimaitijiang M, Sagan V, Sidike P, Hartling S, Esposito F, Fritschi FB (2020) Soybean yield prediction from UAV using multimodal data fusion and deep learning. *Remote Sens Environ* 237:111599
- Manfreda S, McCabe MF, Miller PE, Lucas R, Pajuelo Madrigal V, Mallinis G, Ben Dor E, Helman D, Estes L, Ciraolo G, Müllerová J, Tauro F, de Lima MI, de Lima JLMP, Maltese A, Frances F, Caylor K, Kohv M, Perks M, Ruiz-Pérez G, Su Z, Vico G, Toth B (2018) On the use of unmanned aerial systems for environmental monitoring. *Remote Sens* 10(641):28
- Messina G, Modica G (2020) Applications of UAV thermal imagery in precision agriculture: state of the art and future research outlook. *Remote Sens* 12:1491
- Park S, Ryu D, Fuentes S, Chung H, Hernández-Montes E, O’Connell M (2017) Adaptive estimation of crop water stress in nectarine and peach orchards using high-resolution imagery from an unmanned aerial vehicle (UAV). *Remote Sens* 9:828
- Pepe M, Fregonese L, Scaioni M (2018) Planning airborne photogrammetry and remote-sensing missions with modern platforms and sensors. *Eur J Remote Sens* 51(1):412–436
- Poblete T, Camino C, Beck PSA, Hornero A, Kattenborn T, Saponari M, Bosciae D, Navas-Cortes JA, Zarco-Tejada P (2020) Detection of *xylella fastidiosa* infection symptoms with airborne multispectral and thermal imagery: assessing bandset reduction performance from hyperspectral analysis. *ISPRS J Photogramm Remote Sens* 162:27–40
- Previtali M, Barazzetti L, Redaelli V, Scaioni M, Rosina E (2013) Rigorous procedure for mapping thermal infrared images on three-dimensional models of building façades. *J Appl Remote Sens* 7(1):19
- Ribeiro-Gomes K, Hernández-López D, Ortega JF, Ballesteros R, Poblete T, Moreno MA (2017) Uncooled thermal camera calibration and optimization of the photogrammetry process for UAV applications in agriculture. *Sensors* 7(10):2173
- Santesteban LG, Di Gennaro SF, Herrero-Langreo A, Miranda C, Royo JB, Matese A (2017) High-resolution UAV-based thermal imaging to estimate the instantaneous and seasonal variability of plant water status within a vineyard. *Agric Water Manage* 183:49–59
- Sishodia RP, Ray RL, Singh SK (2020) Applications of remote sensing in precision agriculture: A review. *Remote Sens* 2:3136
- Terentev A, Dolzhenko V, Fedotov A, Eremenko D (2022) Current state of hyperspectral remote sensing for early plant disease detection: a review. *Sensors (Basel)* 22:757
- Tsouros DC, Bibi S, Sarigiannidis PG (2019) A review on UAV-based applications for precision agriculture. *Information* 10(11):349
- Turner D, Lucieer A, Malenovsky Z, King D, Robinson S (2014) Spatial co-registration of ultra-high resolution visible, multispectral and thermal images acquired with a micro-UAV over Antarctic moss beds. *Remote Sens* 6:4003–4024
- Usamentiaga R, Venegas P, Guerediaga J, Vega L, Molleda J, Bulnes FG (2014) Infrared thermography for temperature measurement and non-destructive testing. *Sensors* 14:12305–12348. <https://doi.org/10.3390/s140712305>
- Webster C, Westoby M, Rutter N, Jonas T (2018) Three-dimensional thermal characterization of forest canopies using UAV photogrammetry. *Remote Sens Environ* 209:835–847
- Westoby MJ, Brasington J, Glasser NF, Hambrey MJ, Reynolds JM (2012) Structure-from-motion’ photogrammetry: a low-cost, effective tool for geoscience applications. *Geomorphology* 179:300–314
- Yao H, Qin R, Chen X (2019) Unmanned aerial vehicle for remote sensing applications—a review. *Remote Sens* 11:1443
- Zhang Y, Shi P, Li J (2024) 3D lidar SLAM: a survey. *Photogramm Rec* 39:457–517. <https://doi.org/10.1111/phor.12497>

**Publisher’s note** Springer Nature remains neutral with regard to jurisdictional claims in published maps and institutional affiliations.